Biophysical Properties of a *c*-Type Heme in Chemotaxis Signal Transducer Protein DcrA†

Shiro Yoshioka, Katsuaki Kobayashi, Hideaki Yoshimura, Takeshi Uchida,‡ Teizo Kitagawa, and Shigetoshi Aono*

Okazaki Institute for Integrative Bioscience, National Institutes of Natural Sciences, 5-1, Higashiyama, Myodaiji, Okazaki 444-8787, Japan

Received July 11, 2005; Revised Manuscript Received October 3, 2005

ABSTRACT: Chemotaxis signal transducer protein DcrA from a sulfate-reducing bacterium *Desulfovibrio vulgaris* Hildenborough was previously shown to contain a *c*-type heme in its periplasmic domain (DcrA-N) for sensing redox and/or oxygen [Fu et al. (1994) *J. Bacteriol. 176*, 344−350], which is the first example of a heme-based sensor protein containing a *c*-type heme as a prosthetic group. Optical absorption and resonance Raman spectroscopies indicates that heme *c* in DcrA-N shows a redox-dependent ligand exchange. Upon reduction, a water molecule that may be the sixth ligand of the ferric heme *c* is replaced by an endogenous amino acid. Although the reduced heme in DcrA-N is six-coordinated with two endogenous axial ligands, CO can easily bind to the reduced heme to form CO-bound DcrA-N. Reaction of the reduced DcrA-N with molecular oxygen results in autoxidation to form a ferric state without forming any stable oxygen-bound form probably due to the extremely low redox potential of DcrA-N (−250 mV). Our study supports the initial idea by Fu et al. that DcrA would act as a redox and/or oxygen sensor, in which the ligand exchange between water and an endogenous amino acid is a trigger for signal transduction. While the affinity of CO to DcrA-N (K_d = 138 μM) is significantly weak compared to those of other heme proteins, we suggest that CO might be another physiological effector molecule.

Bacterial heme-based sensor proteins play important roles in various biological events including the regulation of gene expression, chemotaxis, and signal transduction (*1*−*4*). The heme-based sensor proteins studied so far contain a *b*-type heme (iron protoporphyrin IX) to sense gaseous molecules such as oxygen (O_2), nitric oxide (NO), and carbon monoxide (CO) (*1*−*4*). The heme in these sensor proteins is the active site for sensing their effector molecules and regulating their biological functions. The binding of gaseous molecules of the physiological effector to the heme induces a conformational change of the proteins, which is a functional switch of the heme-based sensor proteins (*1*−*4*).

While all of the heme-based sensor proteins well characterized so far contain a *b*-type heme in their active sites, Dolla et al. have reported a putative sensor protein that possesses a *c*-type heme (*5*), a putative chemotaxis signal transducer protein from a sulfate-reducing bacterium *Desulfovibrio vulgaris* Hildenborough, DcrA (*5*). DcrA is thought to consist of a periplasmic N-terminal domain (residues 34−187) and a cytoplasmic C-terminal domain (residues 208−669) with two transmembrane sequences (residues 7−33 and 188−207). The periplasmic N-terminal domain of DcrA contains a Cys-X-X-Cys-His sequence motif (residues 154−158), a common motif to all *c*-type cytochromes. Thus, it has been assumed that DcrA utilizes heme *c* to function (*6*), but the coordination structure of the heme and the function of DcrA have not been elucidated.

Although *c*-type cytochromes are usually involved in electron transfer in many biological systems, DcrA is thought to be a methyl-accepting chemotaxis protein (MCP)[1] responsible for O_2 and/or redox sensing (*7*, *8*). If this is the case, DcrA is the first example of a heme-based sensor protein containing a *c*-type heme as a prosthetic group. There is no example of *c*-type cytochromes that work for O_2 sensing, while *c*-type cytochromes that transiently bind O_2 have been reported previously (*9*−*11*). The mechanism of O_2 and/or redox sensing by a *c*-type heme remain(s) unknown. Therefore, the identification and characterization of *c*-type heme in DcrA are important to understand the structural basis for sensing O_2 and/or the redox potential by *c*-type heme.

In this study, we expressed the periplasmic N-terminal domain of DcrA (DcrA-N, residues 34−191) in *Escherichia*

† This work was supported by a Grant-in-Aid for Scientific Research of Priority Areas on Metal Sensors (Grant 12147203 to S.A.), a Grant-in-Aid for Scientific Research (Grants 16370065 to S.A. and 17770118 to S.Y.) from the Ministry of Education, Culture, Sports, Science, and Technology in Japan, and a grant from the Toray Science Foundation (S.A.).

* To whom correspondence should be addressed. Tel: +81-564-59-5575. Fax: +81-564-59-5576. E-mail: aono@ims.ac.jp.

‡ Present address: Division of Chemistry, Graduate School of Science, Hokkaido University, Sapporo 060-0810, Japan.

[1] Abbreviations: MCP(s), methyl-accepting chemotaxis protein(s); DcrA-N, periplasmic domain of a chemotaxis transducer protein DcrA; TMBZ, 3,3′,5,5′-tetramethylbenzidine; *Ax* PDEA1, *Acetobacter xylinum* phosphodiesterase; *Rm* FixLH, oxygen sensor heme protein from *Rhizobium meliloti*; SW Mb, myoglobin from sperm whale; MA domain, methyl-accepting domain; PAS, acronym formed from the names *Drosophila* period clock protein (PER), vertebrate aryl hydrocarbon receptor nuclear translocator (ARNT), and *Drosophila* single-minded protein (SIM); *Ec* DOS, heme-regulated phosphodiesterase from *Escherichia coli*; HAMP, acronym formed from the names histidine kinase, adenylyl cyclase, methyl-accepting chemotaxis protein, and phosphatase.

10.1021/bi0513352 CCC: $30.25
Published on Web 11/01/2005

coli and characterized its spectroscopic properties using optical absorption, resonance Raman, and redox titration. On the basis of these results, we will discuss biophysical properties of the *c*-type heme and the function of DcrA.

EXPERIMENTAL PROCEDURES

Strains and Plasmids. *D. vulgaris* Hildenborough (NCIMB8303) was obtained from NCIMB. *E. coli* TOP10 (Invitrogen) and JM109(DE3) (Promega) were used for cloning and the expression of DcrA-N, respectively. The pEC86 plasmid containing the *ccmABCDEFGH* genes responsible for the maturation of *c*-type heme proteins was kindly provided by Prof. L. Thöny-Meyer (*12*, *13*). pET-22b(+) was purchased from Novagen.

Construction of an Expression Vector. The *dcrA-N* gene encoding the putative periplasmic domain of DcrA was amplified by polymerase chain reaction (PCR) with the genomic DNA of *D. vulgaris* Hildenborough. The primers were designed to incorporate *Bam*HI and *Xho*I sites at the 5′- and 3′-ends of *dcrA-N*, respectively. The TA cloning kit purchased from Invitrogen was used to subclone the PCR product into a pCR-4 vector to construct pCR-dcrA-N. The DNA fragment containing *dcrA-N* obtained by digesting pCR-dcrA-N with the restriction enzymes, *Bam*HI and *Xho*I, was inserted into the *Bam*HI−*Xho*I site of the pET-22b(+) vector to construct pET-dcrA-N.

The DNA sequences of pCR-dcrA-N and pET-dcrA-N were checked using a DNA sequencer, ABI PRISM 310 genetic analyzer (Applied Biosystems). The N-terminal amino acid sequence was confirmed by a protein sequencer, Procise 494HT (Applied Biosystems).

Expression of DcrA-N. *E. coli* JM109(DE3) was transformed by pET-dcrA-N and pEC86 vectors to construct an expression system. DcrA-N was expressed as follows: 1 mL of an overnight culture of pET-dcrA-N and pEC86/*E. coli* JM109(DE3) was inoculated into 300 mL of Terrific broth (TB) containing ampicillin (final concentration, 50 μg/mL) and chloramphenicol (final concentration, 15 μg/mL) in a 2 L cultivation flask. Cultivation was carried out with a rotary shaker at 180 rpm and 37 °C. About 4 h later, 1 mM IPTG was added to the culture to induce protein synthesis. At the same time, the temperature and shaking speed were set to 22 °C and 140 rpm, respectively, and cultivation was continued for 20 h. The cells were harvested by centrifugation and stored at −80 °C until use.

Purification of DcrA-N. The frozen *E. coli* cells were resuspended in 50 mM potassium phosphate buffer (pH 7.4) containing 0.1 mg/mL phenylmethanesulfonyl fluoride and then sonicated on ice. After centrifugation at 28000 rpm for 20 min, the supernatant was subjected to a HisTrap FF column (Amersham Biosciences) equilibrated with 50 mM potassium phosphate buffer (pH 7.4). The column was washed with 50 mM phosphate buffer containing 10 mM imidazole, and the absorbed protein was eluted with 50 mM potassium phosphate buffer (pH 7.4) containing 200 mM imidazole. The fractions containing DcrA-N were combined and then loaded onto a Resource Q column (Amersham Biosciences) equilibrated with 50 mM Tris-HCl buffer (pH 8.0). The column was extensively washed with 50 mM Tris-HCl buffer (pH 8.0), and the protein was eluted by a gradient of NaCl from 0 to 500 mM. The fractions containing DcrA-N were collected and used for further experiment after exchanging the buffer for 100 mM MOPS buffer (pH 7.0).

The expression and purity of the protein were checked by SDS−PAGE using 15% polyacrylamide gels. The gels were stained by Coomassie Brilliant Blue (CBB) and 3,3′,5,5′-tetramethylbenzidine (TMBZ)/hydrogen peroxide (H_2O_2) for protein and heme staining, respectively. The heme staining of SDS−PAGE gels by TMBZ/H_2O_2 can detect a heme covalently bound to proteins (*14*).

Spectroscopy. Optical absorption spectra were recorded on an Agilent 8453 spectrophotometer (Agilent Technologies) at room temperature. Pyridine hemochrome analysis was performed to determine the type of heme and the protein concentration. The extinction coefficient of 29.1 mM^{-1} cm^{-1} for the 550 nm band of pyridine hemochrome was used to determine the protein concentration (*15*).

Resonance Raman spectra were obtained with a single polychromator (Jobin Yvon, SPEX750M) equipped with a liquid nitrogen-cooled CCD detector (Roper Scientific, Spec10:400LN). The excitation wavelengths were 406.7 and 413.1 nm from a krypton ion laser (Spectra Physics, BeamLok 2060). The laser power at a sample point was adjusted to ∼5 mW for the oxidized and reduced forms and to 0.1 mW for the CO-bound form to prevent photodissociation. Raman shifts were calibrated with indene, CCl_4, acetone, and an aqueous solution of ferrocyanide. The accuracy of the peak positions of well-defined Raman bands was within 1 cm^{-1}. The concentration of the sample was 30 μM in 100 mM MOPS buffer (pH 7.0).

CO Binding Kinetics. The CO association rate (k_{on}) for the reduced DcrA-N was obtained using a stopped-flow spectrophotometer (Unisoku, RSP-1000) under anaerobic condition at room temperature. Reduced DcrA-N (5 μM) (final concentration, 2.5 μM) was mixed with the MOPS buffer (pH 7) containing 0.2−1 mM CO. Formation of the CO-bound complex was monitored at 410 nm. The CO dissociation rate (k_{off}) for the CO-bound form of DcrA-N was determined by NO replacement using a stopped-flow apparatus (*49*). About 8 μM CO-bound DcrA-N (final concentration, 4 μM) was mixed with the NO-saturated MOPS buffer (pH 7). Formation of a six-coordinate, NO-bound DcrA-N was observed under our experimental condition. Dissociation of CO was monitored at 410 nm. We repeated the experiment at least three times for determination of each rate constant. Experimental error for each rate constant was within 15%.

Redox Titration. Redox titration was performed using the method described before (*16*, *17*). The spectral changes of DcrA-N during redox titrations were monitored on an Agilent 8453 spectrophotometer at 15 °C. A gold mesh, platinum wire, and Ag^+/AgCl electrodes were used for working, counter, and reference electrodes, respectively. The protein was dissolved in 100 mM MOPS buffer (pH 7.0) containing 100 mM NaCl as a supporting electrolyte.

RESULTS

The *dcrA-N* gene was fused to the N-terminal signal sequence for periplasmic localization, pelB, in pET-22b(+) to construct pET-dcrA-N. DcrA-N was expressed as a heme protein using pET-dcrA-N with pEC86. Figure 1 shows SDS−PAGE gels stained with CBB (protein staining) and

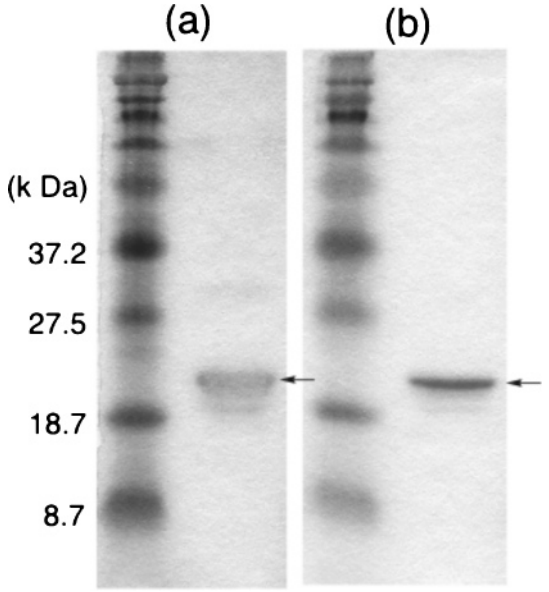

FIGURE 1: SDS−PAGE of purified DcrA-N stained with (a) CBB and (b) TMBZ/H_2O_2. The left lanes for each panel are the molecular mass marker. The arrows in the right lanes in each panel indicate the DcrA-N band.

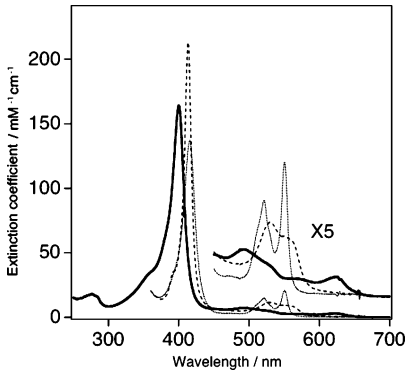

FIGURE 2: Optical absorption spectra of DcrA-N. The bold, dotted, and dashed lines indicate the ferric, ferrous, and ferrous−CO forms of DcrA-N dissolved in 100 mM MOPS buffer at pH 7. The extinction coefficients of the Soret band are 161, 137, and 213 mM^{-1} cm^{-1} for the ferric, ferrous, and ferrous−CO forms, respectively. The spectra between 450 and 700 nm are also plotted with a 5× enlarged scale and a slightly displaced baseline for clarity.

TMBZ/H_2O_2 (heme staining), respectively. The gel stained with CBB showed a band around 20 kDa for DcrA-N, which indicated more than 90% purity for DcrA-N. The band of the purified sample was stained with TMBZ/H_2O_2, which is consistent with the reported result that a *c*-type heme exists in DcrA-N (*6*). The observed molecular mass was consistent with the calculated value of DcrA-N (19.9 kDa).

The N-terminal amino acid sequence of the purified DcrA-N was MDIGINSDPQRQ (data not shown), identical to the expected sequence based on pET-dcrA-N. The first nine residues of the above sequence are derived from the vector pET-22b(+). The first residue encoded by *dcrA-N* is Gln34, which is shown underlined in the above sequence.

DcrA-N showed the typical optical absorption spectra of heme proteins shown in Figure 2. The heme type in DcrA-N was determined by pyridine hemochrome analysis. Pyridine hemochrome derived from DcrA-N showed an α-band at 550 nm typical of *c*-type hemes, showing the presence of a *c*-type heme in DcrA-N. This is consistent with the presence of a *c*-type heme in DcrA-N as DcrA-N on SDS−PAGE gels can be stained by TMBZ/H_2O_2 (heme staining).

Table 1: CO Association and Dissociation Constants for Various Heme Proteins

protein	k_{on} (μM^{-1} s^{-1})	k_{off} (s^{-1})	K_d (μM)[a]	ref
DcrA-N	0.021	2.9	138	this work
Ax PDEA1	0.21	0.058	0.28	*50*
Rm FixLH	0.017	0.083	4.9	*51*
SW Mb	0.51	0.019	0.037	*52*

[a] The K_d value was calculated from k_{on} and k_{off} values.

Optical absorption spectra for purified DcrA-N at pH 7.0 are shown in Figure 2. The ferric DcrA-N showed Soret peak at 400 nm and weak bands at 492 and 624 nm (solid line). While this spectrum is distinct from typical *c*-type cytochromes with His/Met coordination in the ferric form, it is very similar to the ferric forms of the Met80-Ala (M80A) mutant of cytochrome *c* at acidic pH (*18*−*20*) and of *Rhodopseudomonas sphaeroides* heme protein (SHP) at pH 7.0 (*9*). The extinction coefficient of the Soret band at 400 nm was 161 mM^{-1} cm^{-1}, almost identical to that of the M80A mutant of cytochrome *c* (Soret band, 400 nm; extinction coefficient, 164.4 mM^{-1} cm^{-1}) (*19*). When the protein was dissolved in pH 10 buffer, the Soret maximum was red shifted by 1 nm, concomitant with a slight increase and decrease in the absorbance around 530 and 624 nm, respectively (data not shown). This observation indicates that spin state transition from the high-spin to low-spin state occurred by increasing the pH.

The reduction of ferric DcrA-N with a small excess of sodium dithionite gave a Soret band at 416 nm and two resolved bands at 521 and 550.5 nm (Figure 2, dotted line), typical of reduced *c*-type cytochromes with a six-coordinated, low-spin state.

Unlike most *c*-type cytochromes, the addition of CO to reduced DcrA-N generated the CO-bound form with absorption bands at 413, 531, and 556 nm (Figure 2, dashed line). This spectrum is very similar to that of a six-coordinated heme *c*−CO complex with an axial histidine ligand (*26*). The CO association rate constant (k_{on}) for the reduced DcrA-N determined by the stopped-flow method was 0.021 μM^{-1} s^{-1}, and the CO dissociation rate constant was 2.9 s^{-1} (Figures S1 and S2; see Supporting Information). The K_d value for the CO binding to DcrA-N was calculated to be 138 μM, which is quite larger than those of various heme proteins (Table 1). When the reduced DcrA-N reacted with O_2, it formed ferric DcrA-N by autoxidation. No stable O_2-bound form was observed.[2]

To characterize the spin state and coordination structure of *c*-type heme in DcrA-N in detail, we measured the resonance Raman spectra of DcrA-N. Resonance Raman spectra in the high-frequency region of the ferric, ferrous, and CO-bound forms of DcrA-N are shown in Figure 3A,

[2] In the presence of excess sodium dithionite, the reaction of the reduced DcrA-N with O_2 generated a new absorption band at 644 nm, which would show heme degradation. As the reaction of reduced DcrA-N with hydrogen peroxide also resulted in the appearance of the 644 nm band, we concluded that "coupled oxidation" occurred under these experimental conditions. The addition of a small amount of catalase inhibited the appearance of the 644 nm band, consistent with this interpretation (*40*, *41*).

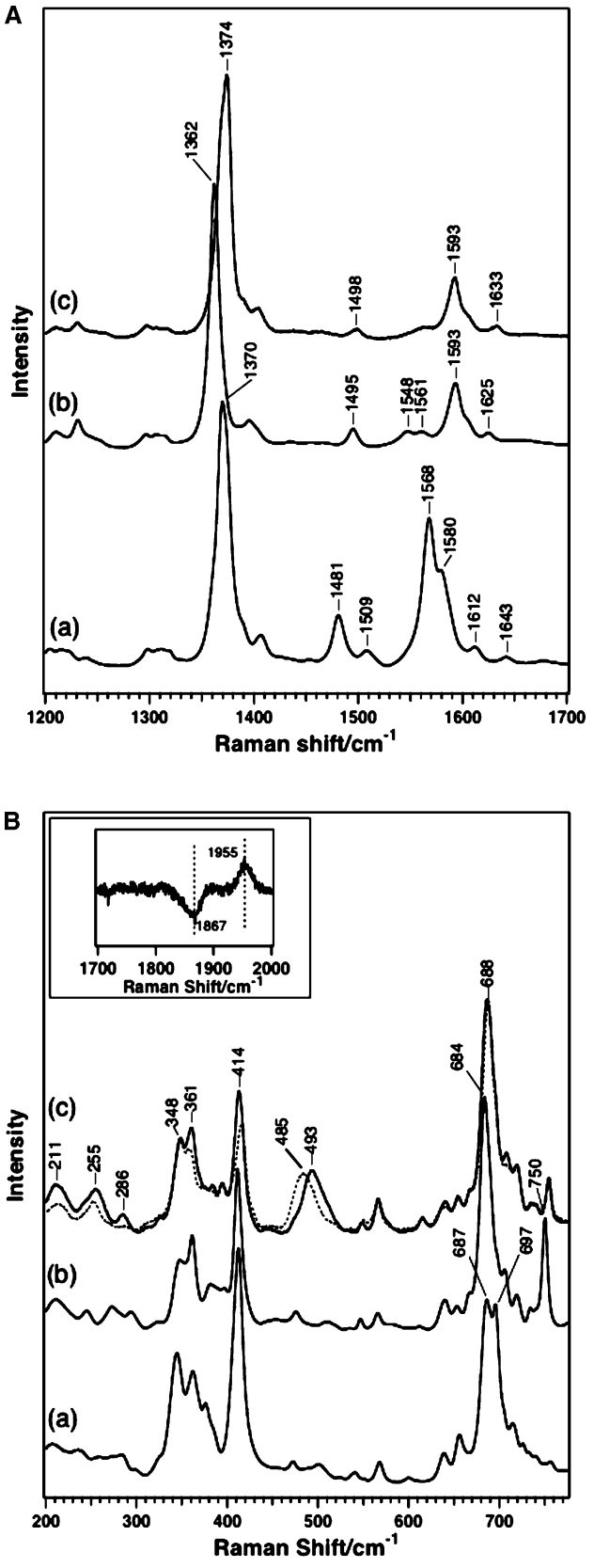

FIGURE 3: Resonance Raman spectra in high- (panel A) and low-frequency (panel B) regions of DcrA-N. The spectra of the ferric and ferrous forms were obtained with laser excitation at 406.7 nm. The spectra for the CO adduct were obtained with 413.1 nm laser excitation. Traces a, b, and c represent ferric, ferrous, and ferrous−CO forms, respectively. The dotted line in trace c of panel B is the $^{13}C^{18}O$-bound form. The inset in panel B shows the difference spectrum between $^{12}C^{16}O$ and $^{13}C^{18}O$ in the C−O stretching region.

and the assignments of the observed frequencies of the heme skeletal modes are summarized in Table 2.

The resonance Raman spectrum of ferric DcrA-N afforded two sets of the heme core marker lines except for the ν_4 line (trace a of Figure 3A). The main species with Raman lines at 1481 cm^{-1} (ν_3), 1568 cm^{-1} (ν_2), and 1612 cm^{-1} (ν_{10}) can be assigned to a six-coordinate, high-spin heme. The Raman lines of the minor component at 1509 cm^{-1} (ν_3), 1580 cm^{-1} (ν_2), and 1643 cm^{-1} (ν_{10}) are similar to those for the six-coordinate, low-spin heme of cytochrome *c* (*22*, *23*). The intensity of the ν_3 line at 1509 cm^{-1} for a low-spin species increased when DcrA-N was dissolved in pH 10 buffer (data not shown). These results are consistent with the results of optical absorption spectra, suggesting that the sixth ligand of the ferric protein was a water or hydroxide ion.

As shown in trace b of Figure 3A, the reduced DcrA-N showed heme core marker lines at 1362 cm^{-1} (ν_4), 1495 cm^{-1} (ν_3), 1593 cm^{-1} (ν_2), and 1625 cm^{-1} (ν_{10}) typical for six-coordinate, low-spin hemes (*22*, *23*). For the reduced form of *c*-type cytochromes, the ν_{11} mode is used to evaluate the electronic nature of the axial heme ligands (*24*, *25*). When a negatively charged ligand such as imidazolate binds to the heme iron, the ν_{11} line shifts to a lower frequency (*24*, *25*). The ν_{11} line at 1548 cm^{-1} for reduced DcrA-N is similar to that of cytochrome *c*, suggesting that neutral ligands bind to the ferrous heme.

The resonance Raman spectrum of the CO complex is shown in trace c of Figure 3A. The ν_4 line at 1374 cm^{-1} and other heme core marker lines at 1498 cm^{-1} (ν_3), 1593 cm^{-1} (ν_2), and 1633 cm^{-1} (ν_{10}) are typical of a CO-bound, six-coordinate heme *c* (*21*, *26*).

Resonance Raman spectra in the low-frequency region are shown in Figure 3B. Strong Raman lines at 414 and 684−688 cm^{-1} were prominent for each spectrum of DcrA-N. For cytochrome *c*, the pairs of Raman lines at 413/421 cm^{-1} and 682/692 cm^{-1} were assigned to $\delta(C_\beta-C_a-C_b)$ and $\nu(C_a-S)$, respectively (*22*, *23*). DcrA-N also showed these Raman lines, indicating the presence of covalent bonds between heme vinyl groups and two cysteine residues.

We observed an isotope-sensitive Raman line at 493 cm^{-1} for the CO-bound form of DcrA-N (traces c of Figure 3B). This Raman line shifted to 485 cm^{-1} when $^{13}C^{18}O$ was used (traces c, dashed line), indicating that this band can be assigned as ν(Fe−CO). The ν(Fe−CO) stretching frequency of DcrA-N suggests that a distal His stabilizing iron-bound CO does not exist in this case. The ν(C−O) line was observed at 1955 cm^{-1} in the high-frequency region of the resonance Raman spectrum (inset of Figure 3B). These two values on the Fe−CO moiety, ν(Fe−CO) and ν(C−O), can be used to obtain information on the axial ligand of CO-bound heme and the heme environmental structure (*27*). The data point of CO-bound DcrA-N falls slightly below the correlation line that the CO adducts of *b*-type hemes with a neutral histidine ligand show, as shown in Figure 4. The axial ligand of CO-bound DcrA-N is thought to be a His, probably His158 in the Cys-X-X-Cys-His motif. Such deviation from the correlation line implies that the proximal His ligand has an anionic character when CO binds to the heme iron. Hydrogen bonding from a surrounding amino acid to the proximal His would make it anionic.

As redox potential is an important factor regulating the function of heme proteins, the redox potential of DcrA-N

Table 2: Observed Frequencies of Heme Skeletal Modes for DcrA-N and Comparisons with Related Proteins

	ν_4	ν_3	ν_2	ν_{10}	heme ligation	ref
Fe^{3+}						
DcrA-N	1370	1481	1568	1612	6cHS(His/water)	this study
		1509	1580	1643	6cLS(His/OH^-)	this study
cyt *c*	1371	1501	1585	1635	6cLS(His/Met)	*22*
cyt *c* folding intermediate	1369	1483	1571		6cHS(His/water)	*42*
myoglobin	1370	1481	1563	1620	6cHS(His/water)	*43*
Fe^{2+}						
DcrA-N	1362	1495	1593	1625	6cLS(His/L)[a]	this study
cyt *c*	1362	1492	1594	1623	6cLS(His/Met)	*22*
$Fe^{2+}-CO$						
DcrA-N	1374	1498	1593	1633	6cLS(His/CO)	this study
cyt *c*′	1371	1467	1591		6cLS(His/CO)	*21*

[a] The unidentified sixth ligand of the ferrous heme is indicated as L.

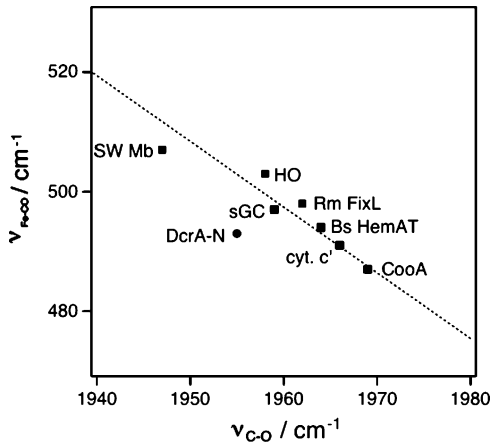

FIGURE 4: Correlation plot between ν(Fe−CO) and ν(C−O). The circle and squares represent the data of DcrA-N and a variety of heme proteins with a proximal histidine, respectively. The data points except for DcrA-N were obtained from refs *26* and *43*−*48*.

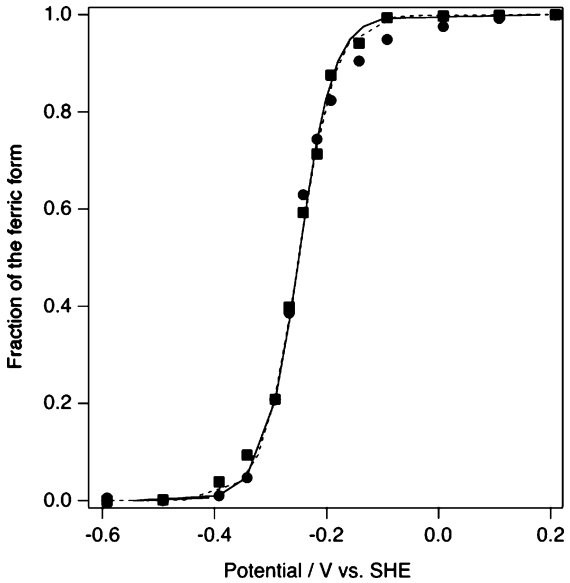

FIGURE 5: Electrochemical redox titrations of DcrA-N. The closed squares and circles represent the data points in reductive and oxidative titrations, respectively. The solid and dashed lines are theoretical curve fittings with the Nernst equation for reductive and oxidative titrations, respectively. The titrations were performed at 15 °C in 100 mM MOPS buffer at pH 7 containing 100 mM NaCl as the supporting electrolyte.

was determined by electrochemical redox titration (Figure 5). The oxidative and reductive titration curves were superimposable, and the redox potential of DcrA-N at pH 7.0 was determined as −250 mV (vs standard hydrogen electrode). While this redox potential is extremely low compared with that of cytochrome *c* (+260−280 mV) (*28*), some *c*-type cytochromes such as *Shewanella putrefaciens* cytochrome c_3 (−233 mV) (*29*), *D. vulgaris* cytochrome c_3 (−242 to −358 mV) (*30*, *31*), and cytochrome c_{550} (−260 mV) (*32*) show a similar redox potential.

DISCUSSION

Genome analysis of *D. vulgaris* Hildenborough reveals the presence of 27 MCPs in its genome, showing that this bacterium has a variety of sensory systems for chemotaxis toward external signals (*33*). DcrA is one of these MCPs and is thought to have periplasmic and cytoplasmic domains with two membrane-spanning regions, which is the common architecture of typical MCPs. As the periplasmic domain of MCPs is responsible for sensing external signals, DcrA-N (the periplasmic domain of DcrA) acts as a sensor for an external signal. Fu et al. previously showed that DcrA contains a *c*-type heme by labeling with 5-amino-[4-^{14}C]-levulinic acid, immunoprecipitation, and autoradiography (*6*). In addition, they found that the methylation levels of the C-terminal methyl-accepting (MA) domain decreased upon addition of oxygen and increased upon subsequent addition of sodium dithionite, as expected for a redox- or oxygen-dependent sensor of the MCP family (*6*). Thus, DcrA has been assumed to utilize heme *c* as a sensor of redox and/or oxygen (*6*). In this study, we characterized the coordination structure, spin state, and reactivity of this *c*-type heme. On the basis of our observations, we discuss the unusual structural properties and function of heme *c* in DcrA.

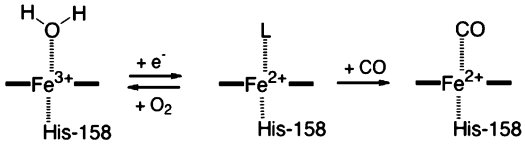

FIGURE 6: Proposed coordination structure of heme *c* in DcrA-N. The unidentified sixth ligand of the ferrous form is indicted as L.

As summarized in Figure 6, we found that heme *c* of DcrA-N shows a unique coordination structure and redox-dependent ligand exchange. While the reduced DcrA-N is six-coordinate with two endogenous axial ligands as is the case in typical *c*-type cytochromes, the coordination structure of the ferric heme in DcrA-N is different from that of typical *c*-type cytochromes. On reduction, a water molecule coordinated to the ferric heme is replaced by an endogenous

amino acid yet unidentified. This redox-dependent ligand exchange is very similar to that observed for DOS from *E. coli* as discussed below.

Ec DOS is a heme-based sensor protein and heme-regulated phosphodiesterase whose activity is regulated by the oxidation state of the heme iron (*34*, *35*). Ferric *Ec* DOS is the inactive form in which a water molecule and His-77 are the axial ligands of the ferric heme. A water molecule coordinated to the ferric heme in *Ec* DOS is replaced by Met-95 on reduction (*35*). In the active form of *Ec* DOS, His77 and Met95 are the axial ligands of the ferrous heme. This ligand exchange between water and Met95 is a trigger of *Ec* DOS activation (*34*, *35*). Thus, the heme in *Ec* DOS acts as a redox sensor regulating enzymatic activity. The redox signal sensed by the heme in *Ec* DOS is transformed to a conformational change of the protein triggered by the redox-dependent ligand exchange.

Reduced DcrA-N converts to the ferric form on reaction with O_2. Autoxidation proceeds very easily, and no stable O_2-bound form is formed, probably due to the low redox potential and the absence of distal amino acid that stabilizes heme-bound O_2. These results indicate that DcrA does not sense O_2 directly. Given the close similarity between DcrA and *Ec* DOS in the redox-dependent ligand exchange, DcrA would be a redox and/or oxygen sensor, but not a direct oxygen sensor.

It is known that *D. vulgaris* Hildenborough shows aerotaxis toward very low oxygen concentration (~0.04%) (*53*). Given that DcrA is responsible for this aerotaxis, the *c*-type heme with very low redox potential will be suitable for sensing very low concentration of O_2. The redox potential of heme *c* would be modulated to be extremely low for the heme to be easily oxidized at low concentration of oxygen. The oxidation of heme *c* would be transmitted to the Che proteins such as CheA, CheW, and CheY through the MA domain of DcrA, resulting in the aerotaxis response of *D. vulgaris*. Our current data are consistent with the initial idea by Fu et al., who proposed that DcrA is a redox and/or oxygen sensor (*5*).

Reduced DcrA-N shows unique reactivity toward CO. Although reduced heme in DcrA-N is six-coordinate with no vacant site for an external ligand, CO can easily bind to the heme to form the CO-bound form. Resonance Raman spectroscopy reveals that an unidentified ligand L (Figure 6) is replaced by CO. This behavior is very similar to that of CooA, a heme-based CO sensor protein. For CooA, one of the axial ligands in the ferrous heme is replaced by CO, a trigger of the CO-dependent activation of CooA (*1*, *2*). The replacement of the axial ligand with CO induces a conformational change to activate CooA. A conformational change will be induced on CO binding also for DcrA.

These results are consistent with the proposed role of DcrA as a redox and/or oxygen sensor. However, as discussed above, it is possible that CO is a physiological effector of DcrA. It is known that *D. vulgaris* Hildenborough metabolizes and produces CO (*36*). Genome analysis reveals that *D. vulgaris* possesses a hydrogen production system from CO, where the membrane-bound hydrogenase (*cooMKLXUHF*) and CO dehydrogenase (DVU2098) could be involved (*33*, *36*). Recently, the CooA homologue (*Dv* CooA) that regulates the CO dehydrogenase expression was also identified in *D. vulgaris* (*37*). The presence of the *coo* operons suggests that *D. vulgaris* can gain energy for growth from CO metabolism, as does *R. rubrum* (*38*). In this case, it makes sense that *D. vulgaris* has a sensor responsible for chemotaxis toward CO. Given that DcrA needs to sense enough concentration of CO for energy metabolism, it also makes sense that DcrA has a low affinity toward CO (K_d = 138 μM). DcrA might be a possible candidate of signal transducer protein that senses CO as an attractant. This remains a hypothesis at present, but is very attractive.

Our current study suggests that heme *c* in DcrA would primarily work as a sensor of redox and/or oxygen for chemotaxis. However, we note that DcrA has a PAS domain in its cytoplasmic domain (*8*). Our preliminary result indicates that the PAS domain does not contain any cofactor such as heme or flavin (Yoshioka and Aono, unpublished results). Since the PAS domain is usually found in many sensor proteins (*8*), it is natural to assume that the PAS domain of DcrA may work for the output of the signal sensed by heme *c*. Thus, one can assume that there might exist a cytoplasmic protein that interacts with the PAS domain of DcrA to transmit the external signal sensed by heme *c* to the cytoplasm. The roles of the PAS domain in DcrA remain to be clarified. While our study is not enough to give a clue to the function of DcrA, chemotaxis assay toward CO and further research on the roles of DcrA in CO sensing and metabolism in this organism will also be required.

ACKNOWLEDGMENT

We thank L. Thöny-Meyer for providing plasmid pEC86. We also thank Y. Makino (NINS) for amino acid sequence analyses.

SUPPORTING INFORMATION AVAILABLE

Two figures showing determination of the CO association rate (k_{on}) for DcrA and the CO dissociation rate (k_{off}) for DcrA-N. This material is available free of charge via the Internet at http://pubs.acs.org.

REFERENCES

1. Aono, S., and Nakajima, H. (1999) Structure and function of CooA, a novel transcriptional regulator containing a *b*-type heme as a CO sensor, *Coord. Chem. Rev. 190*−*192*, 267−282.
2. Aono, S. (2003) Biochemical and biophysical properties of the CO-sensing transcriptional activator CooA, *Acc. Chem. Res. 36*, 825−831.
3. Rodgers, K. R. (1999) Heme-based sensors in biological systems, *Curr. Opin. Chem. Biol. 3*, 158−167.
4. Jain, R., and Chan, M. K. (2003) Mechanisms of ligand discrimination by heme proteins, *J. Biol. Inorg. Chem. 8*, 1−11.
5. Dolla, A., Fu, R., Brumlik, M. J., and Voordouw, G. (1992) Nucleotide sequence of *dcrA*, a *Desulfovibrio vulgaris* Hildenborough chemoreceptor gene, and its expression in *Escherichia coli*, *J. Bacteriol. 174*, 1726−1733.
6. Fu, R., Wall, J. D., and Voordouw, G. (1994) DcrA, a *c*-type heme-containing methyl-accepting protein from *Desulfovibrio vulgaris* Hildenborough, senses the oxygen concentration or redox potential of the environment, *J. Bacteriol. 176*, 344−350.
7. Deckers, H. M., and Voordouw, G. (1994) Identification of a large family of genes for putative chemoreceptor proteins in an ordered library of the *Desulfovibrio vulgaris* Hildenborough genome, *J. Bacteriol. 176*, 351−358.
8. Taylor, B. L., and Zhulin, I. G. (1999) PAS domain: internal sensors of oxygen, redox potential, and light, *Microbiol. Mol. Biol. Rev. 63*, 479−506.

9. Meyer, T. E., and Cusanovich, M. A. (1985) Soluble cytochrome composition of the purple phototrophic bacterium, *Rhodopseudomonas sphaeroides* ATCC17023, *Biochim. Biophys. Acta 807*, 308−319.
10. Gaul, D. F., Gray, G. O., and Knaff, D. B. (1983) Isolation and characterization of two soluble heme *c*-containing proteins from *Chromatium vinosum*, *Biochim. Biophys. Acta 723*, 333−339.
11. Leys, D., Backers, K., Meyer, T. E., Hagen, W. R., Cusanovich, M. A., and Van Beeumen, J. J. (2000) Crystal structures of an oxygen-binding cytochrome *c* from *Rhodobacter sphaeroides*, *J. Biol. Chem. 275*, 16050−16056.
12. Arslan, E., Schulz, H., Zufferey, R., Künzler, P., and Thöny-Meyer, L. (1998) Overproduction of the *Bradyrhizobium japonicum c*-type cytochrome subunits of the cbb_3 oxidase in *Escherichia coli*, *Biochem. Biophys. Res. Commun. 251*, 744−747.
13. Thöny-Meyer, L., Künzler, P., and Hennecke, H. (1996) Requirements for maturation of *Bradyrhizobium japonicum* cytochrome c_{550} in *Escherichia coli*, *Eur. J. Biochem. 235*, 754−761.
14. Goodhew, C. F., Brown, K. R., and Pettigrew, G. W. (1986) Heme staining in gels, a useful tool in the study of bacterial *c*-type cytochromes, *Biochim. Biophys. Acta 852*, 288−294.
15. Drabkin, D. L. (1942) Spectrophotometric studies. X. Structural interpretation of the spectra of cyanide, pyridine, and carbon monoxide derivatives of cytochrome *c* and hemoglobin, *J. Biol. Chem. 146*, 605−617.
16. Nakajima, H., Honma, Y., Tawara, T., Kato, T., Park, S.-Y., Miyatake, H., Shiro, Y., and Aono, S. (2001) Redox properties and coordination structure of the heme in the CO-sensing transcriptional activator CooA, *J. Biol. Chem. 276*, 7055−7061.
17. Inagaki, S., Masuda, C., Akaishi, T., Nakajima, H., Yoshioka, S., Ohta, T., Pal, B., Kitagawa, T., and Aono, S. (2005) Spectroscopic and redox properties of a CooA homologue from *Carboxydothermus hydrogenoformans*, *J. Biol. Chem. 280*, 3269−3274.
18. Raphael, A. L., and Gray, H. B. (1991) Semisynthesis of axial-ligand (position 80) mutants of cytochrome *c*, *J. Am. Chem. Soc. 113*, 1038−1040.
19. Bren, K. L., and Gray, H. B. (1993) Structurally engineered cytochromes with novel ligand-binding sites: oxy and carbon monoxy derivatives of semisynthetic horse heart Ala80 cytochrome *c*, *J. Am. Chem.* Soc. *115*, 10382−10383.
20. Lu, Y., Casimiro, D. R., Bren, K. L., Richards, J. H., and Gray, H. B. (1993) Structurally engineered cytochromes with unusual ligand-binding properties: Expression of *Saccharomyces cerevisiae* Met-80 → Ala iso-1-cytochrome *c*, *Proc. Natl. Acad. Sci. U.S.A. 90*, 11456−11459.
21. Hobbs, J. D., Larsen, R. W., Meyer, T. E., Hazzard, J. H., Cusanovich, M. A., and Ondrias, M. R. (1990) Resonance Raman characterization of *Chromatium vinosum* cytochrome *c*′: Effect of pH and comparison of equiribrium and photolyzed carbonmonoxide species, *Biochemistry 29*, 4166−4174.
22. Hu, S., Morris, I. K., Singh, J. P., Smith, K. M., and Spiro, T. G. (1993) Complete assignment of cytochrome-*c* resonance Raman-spectra via enzymatic reconstitution with isotopically-labeled hemes, *J. Am. Chem. Soc. 115*, 12446−12458.
23. Desbois, A. (1994) Resonance Raman spectroscopy of *c*-type cytochromes, *Biochimie 76*, 693−707.
24. Desbois, A., and Lutz, M. (1992) Redox control of proton transfers in membrane *b*-type cytochromes—an absorption and resonance Raman study on bis(imidazole) and bis(imidazole) model complexes of iron-protoporphyrin, *Eur. Biophys. J. 20*, 321−335.
25. Gao, F., Qin, H., Knaff, D. B., Zhang, L., Yu, L., Yu, C. A., and Ondrias, M. R. (1998) Q-band resonance Raman spectra of oxidized and reduced mitochondrial bc_1 complexes, *Biochemistry 37*, 9751−9758.
26. Andrew, C. R., Green, E. L., Lawson, D. M., and Eady, R. R. (2001) Resonance Raman studies of cytochrome *c*′ support the binding of NO and CO to opposite sides of the heme: implications for ligand discrimination in heme-based sensors, *Biochemistry 40*, 4115−4122.
27. Spiro, T. G., and Wasbotten, I. H. (2005) CO as a vibrational probe of heme protein active sites, *J. Inorg. Biochem. 99*, 34−44.
28. Battistuzzi, G., Borsari, M., Cowan, J. A., Eicken, C., Loschi, L., and Sola, M. (1999) Redox chemistry and acid−base equilibria of mitochondrial plant cytochromes *c*, *Biochemistry 38*, 5553−5562.
29. Tsapin, A. I., Nealson, K. H., Meyers, T., Cusanovich, M. A., Van Beuumen, J., Crosby, L. D., Feinberg, B. A., and Zhang, C. (1996) Purification and properties of a low-redox-potential tetraheme cytochrome c_3 from *Shewanella putrefaciens*, *J. Bacteriol. 178*, 6386−6388.
30. Takayama, Y., Harada, E., Kobayashi, R., Ozawa, K., and Akutsu, H. (2004) Roles of noncoordinated aromatic residues in redox regulation of cytochrome c_3 from *Desulfovibrio vulgaris* Miyazaki F, *Biochemistry 43*, 10859−10866.
31. Ozawa, K., Takayama, Y., Yasukawa, F., Ohmura, T., Cusanovich, M. A., Tomimoto, Y., Ogata, H., Higuchi, Y., and Akutsu, H. (2003) Roles of the aromatic ring of Tyr43 in tetraheme cyotochrome c_3 from *Desulfovibrio vulgaris* Miyazaki F, *Biophys. J. 85*, 3367−3374.
32. Roncel, M., Boussac, A., Zurita, J. L., Bottin, H., Sugiura, M., Kirilovsky, D., and Ortega, J. M. (2003) Redox properties of the photosystem II cytochromes b_{559} and c_{550} in the cyanobacterium *Thermosynechococcus elongates*, *J. Biol. Inorg. Chem. 8*, 206−216.
33. Heidelberg, J. H., Seshadri, R., Haveman, S. A., Hemme, C. L., Paulsen, I. T., Kolonay, J. F., Eisen, J. A., Ward, N., Methe, B., Brinkac, L. M., Daugherty, S. C., Deboy, R. T., Dobson, R. J., Durkin, A. S., Madupu, R., Nelson, W. C., Sullivan, S. A., Fouts, D., Haft, D. H., Selengut, J., Peterson, J. D., Davidson, T. M., Zafar, N., Zhou, L., Radune, D., Dimitrov, G., Hance, M., Tran, K., Khouri, H., Gill, J., Utterback, T. R., Feldblyum, T. V., Wall, J. D., Voordouw, G., and Fraser, C. M. (2004) The genome sequence of the anaerobic, sulfate-reducing bacterium *Desulfovibrio vulgaris* Hildenborough, *Nat. Biotechnol. 22*, 554−559.
34. Sasakura, Y., Hirata, S., Sugiyama, S., Suzuki, S., Taguchi, S., Watanabe, M., Matsui, T., Sagami, I., and Shimizu, T. (2002) Characterization of a direct oxygen sensor heme protein from *Escherichia coli*—Effects of the heme redox states and mutations at the heme-binding site on catalysis and structure, *J. Biol. Chem. 277*, 23821−23827.
35. Kurokawa, H., Lee, D.-S., Watanabe, M., Sagami, I., Mikami, B., Raman, C. S., and Shimizu, T. (2004)A redox-controlled molecular switch revealed by the crystal structure of a bacterial heme PAS sensor, *J. Biol. Chem. 279*, 20186−20193.
36. Voordouw, G. (2002) Carbon monoxide cycling by *Desulfovibrio vulgaris* Hildenborough, *J. Bacteriol. 184*, 5903−5911.
37. Youn, H., Kerby, R. L., Conrad, M., and Roberts, G. (2004) Functionally critical elements of CooA-related CO sensors, *J. Bacteriol. 186*, 1320−1329.
38. Kerby, R. L., Ludden, P. W., and Roberts, G. P. (1995) Carbon monoxide-dependent growth of *Rhodospirillum rubrum*, *J. Bacteriol. 177*, 2241−2244.
39. Fu, R., and Voordouw, G. (1997) Targeted gene-replacement mutagenesis of *dcrA*, encoding an oxygen sensor of the sulfate-reducing bacterium *Desulfovibrio vulgaris* Hildenborough, *Microbiology 143*, 1815−1826.
40. Sigman, J. A., Wang, X., and Lu, Y. (2001) Coupled oxidation of heme by myoglobin is mediated by exogenous peroxide, *J. Am. Chem. Soc. 123*, 6945−6946.
41. Avila, C., Huang, H.-w., Damaso, C. O., Lu, S., Moönne-Loccoz, P., and Rivera, M. (2003) Coupled oxidation vs heme oxygenation: Insights from axial ligand mutants of mitochondrial cytochrome b_5, *J. Am. Chem. Soc. 125*, 4103−4110.
42. Yeh, S.-R., Han, S., and Rousseau, D. L. (1998) Cytochrome *c* folding and unfolding: a biphasic mechanism, *Acc. Chem. Res. 31*, 727−736.
43. Takahashi, S., Wang, J., Rousseau, D. L., Ishikawa, K., Yoshida, T., Takeuchi, N., and Ikeda-Saito, M. (1994) Heme-heme oxygenase complex: structure and properties of the catalytic site from resonance Raman scattering, *Biochemistry 33*, 5531−5538.
44. Aono, S., Kato, T., Matsuki, M., Nakajima, H., Ohta, T., Uchida, T., and Kitagawa, T. (2002) Resonance Raman and ligand binding studies of the oxygen-sensing signal transducer protein HemAT from *Bacillus subtilis*, *J. Biol. Chem. 277*, 13528−13538.
45. Kitagawa, T., Nagai, K., and Tsubaki, M. (1979) Assignment of the $Fe-N_\epsilon$(His F8) stretching band in the resonance Raman spectra of deoxy myoglobin, *FEBS Lett. 104*, 376−378.
46. Uchida, T., Ishikawa, H., Takahashi, S., Ishimori, K., Morishima, I., Okubo, K., Nakajima, H., and Aono S. (1998) Heme environmental structure of CooA is modulated by the target DNA binding, *J. Biol. Chem. 273*, 19988−19992.
47. Pal, B., Li, Z., Ohta, T., Takenaka, S., Tsuyama, S., and Kitagawa, T. (2004) Resonance Raman study on synergistic activation of soluble guanylate cyclase by imidazole, YC-1 and GTP, *J. Inorg. Biochem. 98*, 824−832.

48. Miyatake, H., Mukai, M., Adachi, S., Nakamura, H., Tamura, K., Iizuka, T., Shiro, Y., Strange, R. W., and Hasnain, S. S. (1999) Iron coordination structures of oxygen sensor FixL characterized by FeK-edge extended X-ray absorption fine structure and resonance Raman spectroscopy, *J. Biol. Chem. 274*, 23176−23184.
49. Lambright, D. G., Balasubramanian, S., and Boxer, S. G. (1986) Ligand and proton exchange dynamics in recombinant human myoglobin mutants, *J. Mol. Biol. 207*, 289−299.
50. Chang, A. L., Tuckerman, J. R., Gonzalez, G., Mayer, R., Weinhouse, H., Volman, G., Amikam, D., Benziman, M., and Gilles-Gonzalez, M. A. (2001) Phosphodiesterase A1, a regulator of cellulose synthesis in *Acetobacter xylinum*, is a heme-based sensor, *Biochemistry 40*, 3420−3426.
51. Gilles-Gonzalez, N. A., Gonzalez, G., Peruz, M. F., Kiger, L., Marden, M. C., and Poyart, C. (1994) Heme-based sensors, exemplified by the kinase FixL, are a new class of heme protein with distinctive ligand binding and autoxidation, *Biochemistry 33*, 8067−8073.
52. Springer, B. A., Sligar, S. G., Olson, J. S., and Phillips, G. N., Jr. (1994) Mechanisms of ligand recognition in myoglobin, *Chem. Rev. 94*, 699−714.
53. Johnson, M. S., Zhulin, I. G., Gapuman, M.-E. R., and Taylor, B. L. (1997) Oxygen-dependent growth of the obligate anaerobe *Desulfovibrio vulgaris* Hildenborough, *J. Bacteriol. 179*, 5598−5601.

BI0513352